

University of Tasmania Open Access Repository

Cover sheet

Title

Reliability of EEG microstate analysis at different electrode densities during propofol-induced transitions of brain states

Author

K Zhang, W Shi, C Wang, Y Li, Z Liu, T Liu, J Li, X Yan, Q Wang, Z Cao, G Wang

Bibliographic citation

Zhang, K; Shi, W; Wang, C; Li, Y; Liu, Z; Liu, T; et al. (2021). Reliability of EEG microstate analysis at different electrode densities during propofol-induced transitions of brain states. University Of Tasmania. Journal contribution.

https://figshare.utas.edu.au/articles/journal_contribution/Reliability_of_EEG_microstate_analysis_at_different_el_induced_transitions_of_brain_states/22995221

Is published in:

Copyright information

This version of work is made accessible in the repository with the permission of the copyright holder/s under the following,

CC BY 4.0.

Rights statement: © 2021 The Author(s). Published by Elsevier Inc.

If you believe that this work infringes copyright, please email details to: oa.repository@utas.edu.au

Downloaded from University of Tasmania Open Access Repository

Please do not remove this coversheet as it contains citation and copyright information.

University of Tasmania Open Access Repository

Library and Cultural Collections

University of Tasmania

Private Bag 25

Hobart, TAS 7001 Australia

E oa.repository@utas.edu.au

CRICOS Provider Code 00586B | ABN 30 764 374 782

utas.edu.au

1 Reliability of EEG Microstate Analysis at Different Electrode
2 Densities During Propofol-Induced Transitions of Brain States

3 Kexu Zhang^{a,b,c}, Wen Shi^{d,e}, Chang Wang^{a,b,c}, Yamin Li^d, Zhian Liu^{a,b,c}, Tun
4 Liu^{a,b,c,f}, Jing Li^{a,b,c,f}, Xiangguo Yan^{a,b,c}, Qiang Wang^g, Zehong Cao^h, Gang
5 Wang^{a,b,c,*}

6 ^aThe Key Laboratory of Biomedical Information Engineering of Ministry of Education,
7 Institute of Biomedical Engineering, School of Life Science and Technology, Xi'an
8 Jiaotong University, Xi'an, 710049, China

9 ^bNational Engineering Research Center for Healthcare Devices, Guangzhou, 510500,
10 China

11 ^cThe Key Laboratory of Neuro-informatics and Rehabilitation Engineering of Ministry
12 of Civil Affairs, Xi'an, 710049, China

13 ^dSchool of Biomedical Engineering, Shanghai Jiao Tong University, Shanghai 200240,
14 China.

15 ^eThe Key Laboratory for Biomedical Engineering of Ministry of Education, Department
16 of Biomedical Engineering, College of Biomedical Engineering & Instrument Science,
17 Zhejiang University, Hangzhou, 310027, China

18 ^fDepartment of Anesthesiology, Honghui Hospital, Xi'an Jiaotong University, Xi'an,
19 710054, China

20 ^gDepartment of Anesthesiology and Center for Brain Science, The First Affiliated
21 Hospital of Xi'an Jiaotong University, Xi'an 710061, Shaanxi, China

22 ^hSchool of Information and Communication Technology, University of Tasmania,
23 Hobart, TAS, 7001, Australia

24
25 *Corresponding author at: Xi'an Jiaotong University, School of Life Science and
26 Technology, No.28, Xianning West Road, Xi'an, Shaanxi, 710049, P.R. China.

27 E-mail address: ggwang@xjtu.edu.cn (Gang Wang).

Abstract

Electroencephalogram (EEG) microstate analysis is a promising and effective spatio-temporal method that can segment signals into several quasi-stable classes, providing a great opportunity to investigate short-range and long-range neural dynamics. However, there are still many controversies in terms of reproducibility and reliability when selecting different parameters or datatypes.

In this study, five types of electrode configurations (including 91, 64, 32, 19, and 8 channels), were configured to measure the reliability of microstate analysis at different five electrode densities during the propofol-induced sedation.

First, the microstate topography and parameters at different five electrode densities were compared between the baseline (BS) condition and the moderate sedation (MD) condition, respectively. The intraclass correlation coefficient (ICC) and coefficient of variation (CV) were introduced to quantify the consistency of the microstate parameters.

Second, the statistical analysis and classification between BS and MD were performed to determine whether the microstate differences between different conditions can remain stable at different electrode densities, and ICC is also calculated between different condition to measure the consistency of the results in a single condition.

The results showed that either in BS condition or the MD condition, there were few significant differences of microstate parameters among the configurations of 91, 64, and 32 channels, and the majority differences existed between the configurations of 19 and 8 channels and other channels. The ICC and CV also showed that the consistency among the configurations of 91, 64, and 32 channels was better than that among all 5 types of electrode configurations after involving 19 and 8 channels. Furthermore, the significant differences between the conditions in 91 channels remained stable those in 64 and 32 channels, but it disappeared for the conditions in 19 and 8 channels. In addition, the results of classification and ICC showed that the microstate analysis becomes unreliable with less than 20 electrodes.

The findings in this study supports our hypothesis that the microstate analysis of different brain states is more reliable with high electrode densities and it is not

recommended to use with a small number of channels for EEG microstate analysis.

Highlights

- In baseline and moderate sedation conditions, the microstate topography and parameters in the configurations of 91, 64, 32 channels keep the high consistency.
- The microstate characteristics of propofol induction remain outstanding stabilities in the configurations of 91, 64 and 32 channels, excepting the brain scalps with only 19 or 8 channels.
- Our findings imply the microstate analysis is not applicable in the low electrode densities, such as less than 20 EEG channels.

Key words: *Reliability, Microstate analysis, EEG, Propofol-induced sedation, Intraclass correlation coefficient*

1 Introduction

2 Extracting reliable biomarkers is vital to benefit for the diagnosis and treatment of
3 neuropsychiatric illnesses. As a non-invasive and low-cost imaging tool,
4 electroencephalography (EEG) has been widely used to measure the electrical activity
5 of the brain cortex and detect neural dynamic changes within milliseconds, providing a
6 practical and normative reference in the diagnosis of neurophysiological diseases
7 (Fitzgerald and Watson, 2018; Sharmila, 2018). Many existing signal processing
8 methods have been proposed for EEG feature extractions (Gudmundsson et al., 2007),
9 while most of them only focused on exploring specific channels that led to extreme
10 variation between conditions or groups and neglected the overall potential
11 characteristics of the brain cortex. However, monitoring the changes in the temporal
12 configuration of rapidly fluctuating scalp potential maps is important and considered as
13 a practical and emerging approach for early detections of diseases (Milz et al., 2017).
14 Some studies have indicated that the scalp potential map always maintains a particular
15 quasi-stable state, called the microstates (Lehmann et al., 1987) for the period of 60-
16 120ms, and then changes into another state quickly. The corresponding EEG microstate
17 analysis aims to explore large-scale neural networks, which combines the temporal and
18 spatial EEG information to demonstrate the dynamics of the scalp potential topography
19 (Michel and Koenig, 2018). A set of microstates, labeled as A to G (Custo et al., 2017),
20 is generally considered to be the most representative topography, in which of each
21 microstate represents specific neural networks in the resting state (Britz et al., 2010;
22 Musso et al., 2010). Moreover, it was recognized that the changes of cognitive and
23 pathological states are usually associated with the changes of microstate features. For
24 instance, an event-related potential study revealed that microstate topography related to
25 the performance of different tasks (Brandeis et al., 1995), which was used to assist the
26 follow-up studies to find the different microstates dominated at different levels of
27 consciousness (Brodbeck et al., 2012; Katayama et al., 2007). **What is more, the**
28 **changes of microstates are consistant with the learning process and behavior (Koenig**
29 **et al., 2002), while microstate features (i.e., topography, duration, coverage, and**

occurrence) were found to be altered in schizophrenia (Kikuchi et al., 2007; Lehmann et al., 2005; Nishida et al., 2013), semantic dementia (Grieder et al., 2016), head injury (Corradini and Persinger, 2014), Alzheimer's disease (Nishida et al., 2013), stroke (Zappasodi et al., 2017), and panic disorders (Kikuchi et al., 2011). With the evidence from the board clinical applications, the dynamic microstate is a promising biomarker to reveal the underlying relationship between EEG signals and brain activities in changing conditions.

Considering the above influences, it is necessary and worthwhile to study the reliability of the microstate analysis and guarantee the stability of outcomes with different factors. These factors include data lengths, clustering algorithms, the number of clusters, smoothing parameters, and preprocessing strategies, which have the potential to interfere the process of EEG microstate analysis and may cause the negative effects. Wiithin these factors, in particular, the electrode configuration is one of the most important factor needed to be seriously considered in the microstate analysis, as different electrode densities and spatial position may delineate scalp potential topography dynamics in different resolutions and locations. For instance, several studies designed different numbers of electrodes only made a repeated conclusion that the microstate D of schizophrenia patients had a shorter duration, compared to that of normal subjects (Kikuchi et al., 2007; Lehmann et al., 2005; Nishida et al., 2013). One of these studies using 21-channel EEG revealed that the microstate A had a shorter duration (Nishida et al., 2013), while another two studies using 27-channel EEG (Lehmann et al., 2005) or 14-channel EEG (Strelets et al., 2003) did not show the same phenomenon, suggesting that the number of channels may affect the result consistency. In addition, some studies related to the consistency and reliability of the microstate have been carried out as well. For example, the inter-studies and inter-individual consistency of microstate sequence were analysed through five different oral picture naming studies (Laganaro, 2017). In this study, the stability of five different microstate clustering algorithms were compared in terms of metrics: similarity, global explained variance, and entropy changes but there is no significant differences (von Wegner et al., 2018). Another study examined the test-

1 retest reliability of different algorithms, via the k-means clustering and the topographic
2 atomize agglomerate hierarchical clustering, different clustering approaches (global,
3 session, and recording), and different numbers (30, 19, and 8) of channels. The results
4 showed that the global clustering approach could obtain more stable microstates, and
5 these three electrode configurations have demonstrated the high test-retest reliability.
6 (Khanna et al., 2014).

7
8 To the best of our knowledge and surveyed the literatures above, there are no reliability
9 studies present a solid finding for the setting issues of a broad range of channel numbers,
10 and most of related existing studies only focused on the microstate in the resting state
11 (Khanna et al., 2014). Thus, the aim of our study is to investigate the reliability of EEG
12 microstate features at different electrode densities during the overall propofol-induced
13 transition process of brain states. Firstly, the number of channels will be selected in this
14 study ranged from 8 to 91, including the numbers of channels used in the recent study
15 (Michel and Koenig, 2017). Then, we will introduce the methodology of our study,
16 which is mainly divided into two parts. In the first part, the reliability of the microstate
17 is tested in the baseline and the moderate sedation conditions, respectively. For each
18 condition, we examined whether similar microstate topography can be obtained by
19 clustering at five different electrode densities. Then, six types of microstate parameters
20 (including duration, coverage, occurrence, GFP peaks/second, transition probability,
21 and entropy rate), are compared at five electrode densities. The intraclass correlation
22 coefficient (ICC) and coefficient of variation (CV) are used to evaluate the consistency
23 of microstate parameters. In the second part, the reliability of microstate parameter
24 features during the propofol-induced transition process at five electrode densities will
25 be tested. Finally, we will make a brief conclusion and discuss our findings based on
26 the the number of channels recommended for the microstate analysis.

28 **Methods**

29 In this study, we explored the microstate reliability of different electrode densities in

the baseline condition, the microstate reliability of different electrode densities in the moderate sedation condition, and the consistency of features at different electrode densities during the transitions of consciousness. A diagram outlining the data analysis protocol is shown in Fig. 1.

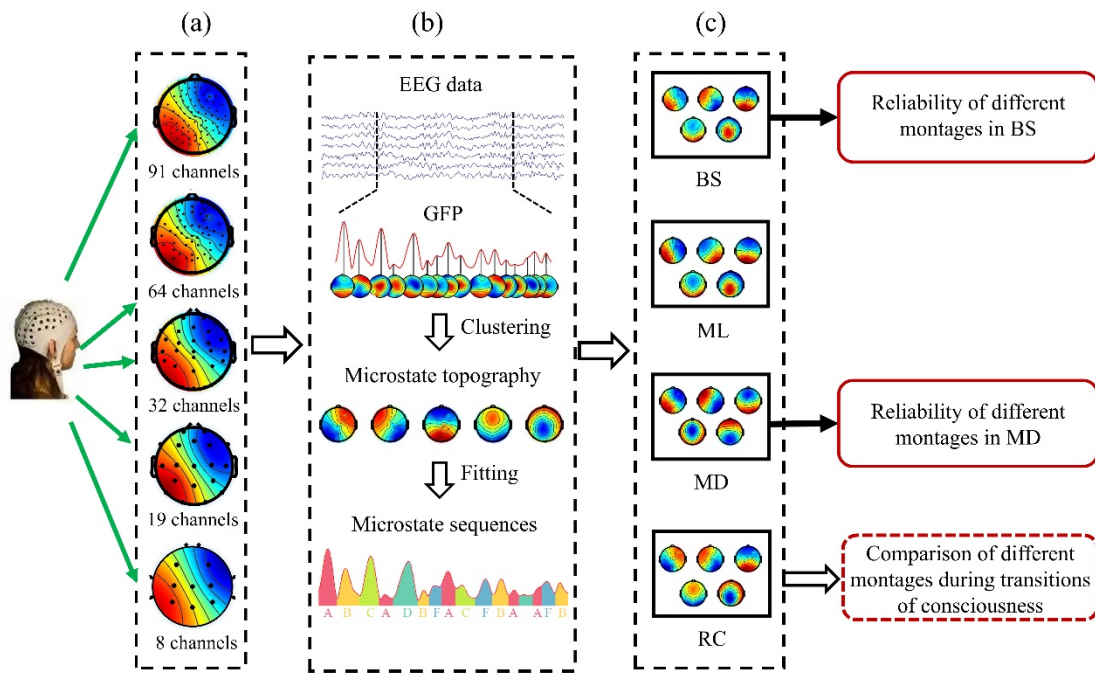


Fig. 1. The protocol of the data analysis. (a) topographic configurations with 5 types of different electrode densities. (b) the illustration of microstate clustering. The GFP curve of the multi-channel EEG is calculated to measure the strength of scalp potential. The EEGs at GFP local maximum points are selected for clustering purpose. The microstates obtained by clustering fit back to the continuous EEG data to obtain the microstate sequences. (c) the whole propofol-induced transition procedure is divided into four conditions: the baseline (BS), the mild sedation (ML), the moderate sedation (MD), and the recovery stage (RC). Please note that the number of clusters is 5, and the optimal number of clusters varies depending on the dataset and the method.

2.1 Data recording and preprocessing

The experimental dataset is obtained from the open-access section in University of Cambridge Data Repository (<https://www.repository.cam.ac.uk/handle/1810/252736>). The dataset contains well-processed EEG data of 20 healthy subjects

(male/female=9/11; mean age=30.85, SD=10.98) during propofol injection. During the experiment, the brain state of the subjects was divided into four conditions: the baseline (BS), the mild sedation (ML), the moderate sedation (MD) and the recovery stage (RC) where each condition lasted approximately 7 minutes. A computerized syringe driver (Alaris Asena PK, Carefusion, Berkshire, UK) was used to control the infusion of propofol and maintain the target concentration. A blood plasma level of 0.6 $\mu\text{g/ml}$ corresponds to the mild sedation, and 1.2 $\mu\text{g/ml}$ corresponds to the moderate sedation. The electrical activity of brain was collected by using a 128-channel EEG amplifier at 250 Hz sampling rate and referenced to the vertex. Each subject had the eyes closed during EEG data collection. All data preprocessing steps were implemented using the EEGLAB toolbox installed in the Matlab. Channels on the neck, cheeks and forehead were excluded, because these channels are more susceptible to movement-related noises. Eventually, there were 91 channels retained for further EEG analysis. The raw data was filtered between 0.5-45 Hz and then segmented into 10-second epochs. The baseline-correction was also made for each epoch, relative to the mean voltage of the epoch. A quasi-automated program was rejected data that contains the excessive eye movement or the muscle artifact by calculating the normalized variance and manually choosing whether to retain it. After removing the epoch with the poor signal quality, each subject had at least 30 epochs in each section for the following EEG analysis (Chennu et al., 2016). By spatially down-sampling from 91 channels of EEG signals to 64, 32, 19, or 8 channels of EEG signals, the newly generated five EEG datasets with different electrode densities were obtained to perform the microstate analysis. Five types of electrode distributions have been configured according to the modified 10-20 system, as illustrated in Fig.1 (a).

2.2 Microstate analysis

The microstate analysis mainly consisted of three steps: clustering, fitting, and the parameter calculation.

The process of clustering and fitting is illustrated in Fig.1 (b). Each sampling point was

analyzed as an independent EEG topography. Global Field Power (GFP) quantifies the strength of scalp potential and is equal to the standard deviation of all channel potentials at each sampling point. The local maximum position of GFP is considered to have the optimal signal-to-noise ratio and the stable topography. Therefore, the maps corresponding to the local maximum of GFP were picked up to conduct the further microstate clustering and fitting (Skrandies, 1990). All selected maps were clustered using the modified k-means algorithm, which is a mature clustering method widely used in many microstate studies (Pascual-Marqui, 1995), and the clustering number was determined by Krzanowski-Lai Criterion (KL) (Murray et al., 2008). Compared with the cross-validation method (Lai, 1988), the KL method is not sensitive to the number of electrodes, so it assume to be suitable for this study. The optimal number of clusters for each condition was based on the KL result of 91-channel data that has been used in exisiting studies (Shi et al., 2020).

<add information> Global explained variance (GEV) is a measure of the degree to which the microstate clustering describes the dataset, and its value ranges between 0 and 1 (Murray et al., 2008): the higher the value, the better the quality of microstate analysis. One characteristic of the modified k-means algorithm is the randomly selected initial template, so the results of multiple calculations may be inconsistent. Therefore, GEV was compared to evaluate the quality of results after clustering. Each clustering process was repeated 100 times, and the maps corresponding to the highest GEV were identified as the final microstates. Additionally, the polarity of maps was disregarded in the clustering computation.

Then, the continuous EEG was labeled by the microstates. For each peak of GFP, the spatial correlation between EEG data and each microstate was calculated, and this sampling point was labeled as the microstate label with the highest correlation. For the data between GFP peaks, the label of each point corresponded to the label of the closet GFP peak. In order to keep microstate label stable for a certain amount of time until it changes, the method of temporal smoothing was employed to eliminate the rapid

change of microstate caused by noises in the microstate sequence. The smoothing algorithm was introduced to reduce rapid microstate changes caused by noises, and the smoothing parameter was set as the window size parameter $b=1$ and the nonsmoothness penalty parameter $\lambda=0.05$.

In order to measure the consistency of the microstate in different electrode densities more comprehensively, the basic parameters and sequence-related parameters were calculated separately. The basic parameters were the parameters calculated by most microstate studies, mainly including GFP peaks per second, duration, coverage, and occurrence. The “**GFP peaks per second**” is the average number of GFP peaks per second. The “**duration**” denotes the average duration of each occurrence of a current microstate before switching to another microstate. The “**coverage**” is the time coverage for each microstate in the whole time series. The “**occurrence**” represents the average times of occurrences per second of each microstate. It is worth mentioning that because of the discontinuity of epoch, the duration of the first and last microstates in each epoch was unknown, so these positions did not participate in the calculation of “duration”, “coverage”, and “occurrence”. The averaged value of all epoch parameters of each subject was used as the final parameters.

Sequence-related parameters are parameters that can reflect the characteristics of a sequence, mainly including “transition probability” and “entropy rate”. The “**transition probability**” reflects the probability of each microstate transforming into another microstate. Transition Probability from A to B is the number of transitions from A to B divided by the number of all transitions from A to other microstates. The “**entropy rate**” is an index to measure the temporal property of microstate sequence, and it quantified how much uncertainty the process produced by increasing the length of the observed “characteristic sequence” (von Wegner et al., 2017). Based on the definition of Shannon entropy, the joint entropy is designed to quantify the entropy value under different microstate sequence lengths. The calculation method of joint entropy is defined as

$$h_n = - \sum_{x_1, \dots, x_n} p(x_1, \dots, x_n) \log p(x_1, \dots, x_n) \quad (1)$$

where h_n represents joint entropy when the characteristic sequence length is n , x_1, \dots, x_n representing a continuous microstate sequence, and $p(x_1, \dots, x_n)$ represents the probability of this particular microstate sequence appears in the entire sequence. The joint entropy value change as the length n of the characteristic sequence changes and the entropy rate is calculated as the slope of the linear least squares fit of n and h_n . Due to the short epoch length, the joint entropy cannot be accurately reflected when the value of n is large. Here, the entropy value of the characteristic sequence length from 1 to 6 is selected to estimate the entropy rate.

2.3 Reliability analysis of EEG microstate

2.3.1 Reliability at different electrode densities in BS condition

In BS condition, five datasets with different electrode densities were analyzed by the above method of microstate analysis and the clustering number was assigned as 4. Five sets of microstate maps and parameters were obtained and further compared. The 91-channel microstate label is visually judged by the results of previous studies (Custo et al., 2017), and the microstate labels at 64, 32, 19, and 8 channels are obtained by Pearson correlation coefficient (PCC). First, PCC between each microstate map in 91 electrodes and each microstate map in 64, 32, 19 and 8 electrodes was computed, the label of each Map matched the label of the 91-channel microstate with the maximum correlation. The higher the PCC, the better the correlation between the two groups of microstates. Since the vector sizes of the two groups of microstates are different, only the electrode group corresponding to the lower electrode density was selected. Second, the analysis of variance (ANOVA) were performed to check whether the electrode density influenced each microstate parameter. For the parameters with significance differences, the Post hoc paired *t-test* with Bonferroni correction for multiple comparisons was conducted to seek further which two groups have significant differences. In addition, the ICC and CV were introduced to quantify the consistency of microstate parameters between five different electrode densities. ICC is a common

indicator to evaluate test re-test and inter-observer reliability (Ip et al., 2018). The ICC grows higher as the intra-class variance grows smaller and the inter-class variance grows larger. The high ICC shows that data from the same class is highly correlated. Considering the characteristic of testing data, we selected the two-way random model to calculate the average absolute agreement (Shrout and Fleiss, 1979). In this part, the parameter values for each subject with all five types of electrode densities were within the class, while the parameter values of different subjects were between classes. The smaller the parameter difference under different electrode densities of the same subject and the greater the parameter difference between different subjects, the higher the ICC. The paired *t-test* was used to examine whether there were ICC differences between various kinds of EEG electrode density combinations. The ICC calculation formula of two-way random model is shown as follows:

$$ICC = \frac{MS_R - MS_E}{MS_R + (MS_c - MS_E) / n} \quad (2)$$

where MS_R represents the mean square for rows, MS_c represents the mean square for columns, and MS_E represents the mean square error. The CV is a measure of dispersion and defined as the standard deviation divided by the mean (Shoukri et al., 2008). In this part, the dispersion of each parameter in five electrode configurations was quantified. When neither the subjects nor the observations were unique, the mean and standard deviation were calculated as follows:

$$\mu = \frac{1}{n * k} \sum_{i=1}^n \sum_{j=1}^k y_{ij} \quad (3)$$

$$\sigma = \frac{1}{n * k} \sum_{i=1}^n \sum_{j=1}^k \left(y_{ij} - \frac{1}{k} \sum_{j=1}^k y_{ij} \right)^2 \quad (4)$$

where Y_{ij} denotes the parameter of the i th subject under the j th configuration, and n represents the number of subjects and k represents the number of configurations.

2.3.2 Reliability among different electrode densities in MD condition

The microstate analysis was performed on five datasets in MD condition, and the clustering number was assigned as 5 (Shi et al., 2020). The PCC of maps between 91 channels and 64, 32, 19, or 8 channels were calculated to test if the microstate maps are

stable under different electrode densities. Each parameter of the microstate was subjected to the same statistical analysis and consistency analysis in the sub-section 2.3.1.

2.3.3 Comparison of different electrode densities during propofol-induced transitions of consciousness

To investigate whether the microstate parameter features at five electrode densities change similarly during propofol-induced transitions of consciousness, the EEG microstate in four conditions was reanalysed with the same clustering number 5. In the previous study, we have found that in the case of 91-channel EEG, there are significant differences for some parameters between BS and MD conditions. Therefore, it is worth to test whether these differences varied with the number of channels. In this study, the coverage of microstate C (Coverage C), the coverage of microstate F (Coverage F), the duration of microstate C (Duration C) and the occurrence of microstate F (Occurrence F) were compared in different electrode densities and paired *t-test* was used to check whether the significant differences could remain stable. Moreover, we performed the statistical analysis (paired *t-test* or Wilcoxon signed rank test, determined by the characteristics of the data) on the Transition Probability and Entropy Rate in the BS and MD states to explore whether the transition trend and complexity of the microstate sequence change with the change of the brain state. Finally, all parameters with significant difference were used as the features to input to a support vector machine (SVM) classifier for distinguishing EEG in BS and MD conditions. The RBF kernel was selected, and the best parameters **c** and **g** were selected by grid optimization. The strategy of leave-one-out cross validation (LOOCV) method was chosen to evaluate the classification results. As each case was tested once, the results were combined to generate a receiver operating characteristic (ROC) curve. Then, the area under curves (AUC) was calculated to quantify the classification performance of LOOCV.

In addition, the consistency during the change-of-consciousness was evaluated by calculating the ICC values between different electrode densities. In this part, all

conditions (BS, ML, MD and RC) of each subject were analyzed separately. The parameter values for the same condition as all five kinds of electrode densities were within the same class. The parameter values for the different conditions were between different classes. The smaller the parameter difference at different electrode densities of the same condition and the greater the parameter difference between different conditions, the higher the ICC.

Results

3.1 Reliability in BS condition

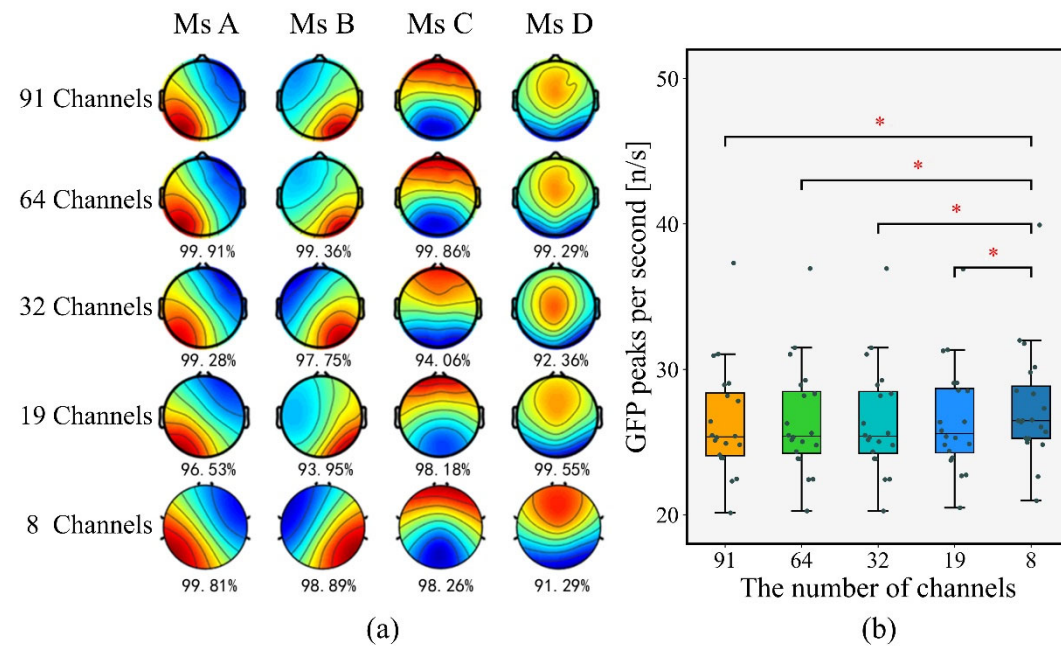


Fig. 2. (a) the topographies of BS microstates at five electrode densities. The maps were labeled as microstates A, B, C and D. The Pearson Correlation coefficients between microstates at 64, 32, 19, or 8 channels and corresponding the microstate at 91 channels were marked under the topographies. (b) boxplots of GFP peaks per second in the BS condition under different electrode densities. The bar of each subgraph is the standard deviation. Ms: Microstate. *: $p < 0.005$ (Bonferroni Corrected).

In BS condition, five sets of microstate maps at different electrode densities are shown

in Fig.2 (a). The range of PCC between microstates at 91-channel configuration and microstates at other configurations is from 0.91 to 0.99. Each set of microstate maps can match the generally accepted microstates A, B, C, and D individually. GFP peaks per second at different configurations were compared in Fig.2 (b). The averaged GFP peaks per second changed between 26.38 and 27.46. There were significant differences between parameters at the 8-channel configuration and parameters at the other configurations.

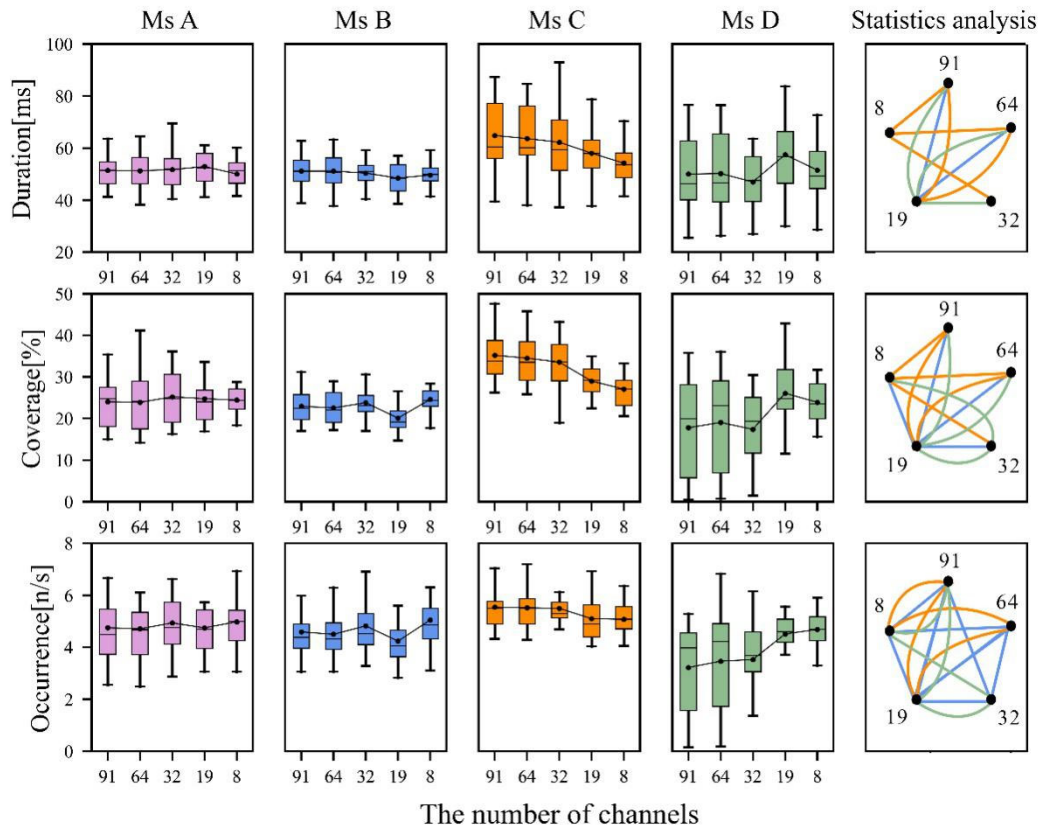


Fig. 3. Group comparison of (a) Duration, (b) Coverage, and (c) Occurrence in the BS condition at different electrode densities. The four columns on the left side are the descriptive graphs of the microstate parameters. The right-most column is the result of statistics analysis. A line between two nodes indicates that these two configuration have the significant difference and the color of line mark the corresponding microstate. The bar of each subgraph is the standard deviation. All statistical differences have been Bonferroni Corrected. The “Ms” is stand for the microstate.

The results of Duration, Coverage, and Occurrence at five electrode densities are

1 illustrated in Fig. 3. From the comparison in the left four columns, it could be shown
2 that these parameters were not as highly consistent as GFP peaks per second. For five
3 datasets with different electrode densities, the microstate analysis results were not
4 completely similar. The right-most column showed statistical analysis results. If there
5 was a line between two nodes, it indicated that there were significant differences
6 between the related two kinds of electrode densities and the line color was concordant
7 with the color of corresponding microstate. For Duration and Coverage, there were no
8 significant differences among 91, 64, and 32 channels. All the differences occurred
9 between 19-channel or 8-channel configurations and the other configurations. For
10 Occurrence, except for the differences between 32-channel configuration and 64-
11 channel, 91-channel configuration in microstate D, the other differences were all from
12 between 19-channel or 8-channel configuration and the other configurations.

13

14 **Table 1** The descriptive summary of ICC and CV of basic parameters in the BS condition

Parameter	Ms	91vs64vs32vs19vs8		91vs64vs32vs19		91vs64vs32	
		ICC	CV	ICC	CV	ICC	CV
Duration	A	0.96	6.02%	0.96	5.38%	0.98	3.54%
	B	0.97	4.70%	0.96	4.57%	0.97	3.69%
	C	0.94	10.37%	0.95	8.80%	0.97	6.22%
	D	0.94	12.92%	0.94	12.52%	0.96	9.16%
Coverage	A	0.92	12.99%	0.95	10.93%	0.96	9.19%
	B	0.89	11.92%	0.9	10.63%	0.93	7.56%
	C	0.69	16.93%	0.74	14.78%	0.85	10.86%
	D	0.87	32.96%	0.9	31.85%	0.94	25.65%
occurrence	A	0.98	8.04%	0.99	6.17%	0.99	5.88%
	B	0.97	9.35%	0.98	7.42%	0.98	5.81%
	C	0.94	7.85%	0.95	6.80%	0.96	5.37%
	D	0.8	30.89%	0.86	29.23%	0.91	24.53%
STD		0.08	9.13%	0.07	9.00%	0.04	7.48%

Average	0.91	13.74%	0.92	12.42%	0.95	9.79%
---------	------	--------	------	--------	------	-------

Table 1 shows the descriptive summary of ICC and CV in BS condition. The consistency of 91 vs. 64 vs. 32 vs. 19 vs. 8 (5 kinds of electrode densities, 5KED), 91vs64vs32vs19(4 kinds of electrode densities, 4KED) and 91vs64vs32(3 kinds of electrode densities, 3KED) in BS condition were calculated respectively. The averaged ICC and CV of 5KED were 0.91 (SD=0.08) and 13.74% (SD=9.13%). The averaged ICC and CV of 4KED were 0.92 (SD=0.07) and 12.42% (SD=9.13%). The averaged ICC and CV of 3KED were 0.95 (SD=0.04) and 9.79% (SD=7.48%). Statistical analysis showed that the ICC of 5KED, 4KED and 3KED were significantly different in pairs. The ICC of 3KED was higher than that of 4KED and 5KED, while the CV had the opposite trend.

The changes in the transition probability of each pair of microstates and the results of statistical analysis are shown in Supplementary Fig. S1. For all 16 different microstate transitions, the difference in parameters mainly existed between 19-channel or 8-channel configuration and other configurations. The ICC and CV of Transition Probability in BS condition are shown in Table S1. On the basis of 3KED, adding 19 channels and 8 channels in sequence would gradually reduce the averaged ICC and increase the CV. The results of Entropy rate in BS condition at different electrode densities are shown in Fig. S2. Entropy rate in BS condition had the same changing trend with GFP peaks per second. When the number of channels was no less than 19, Entropy Rate could remain stable, and when the number of channels is 8, the Entropy Rate was significantly different from the results of the other four configurations.

3.2 Reliability in MD condition

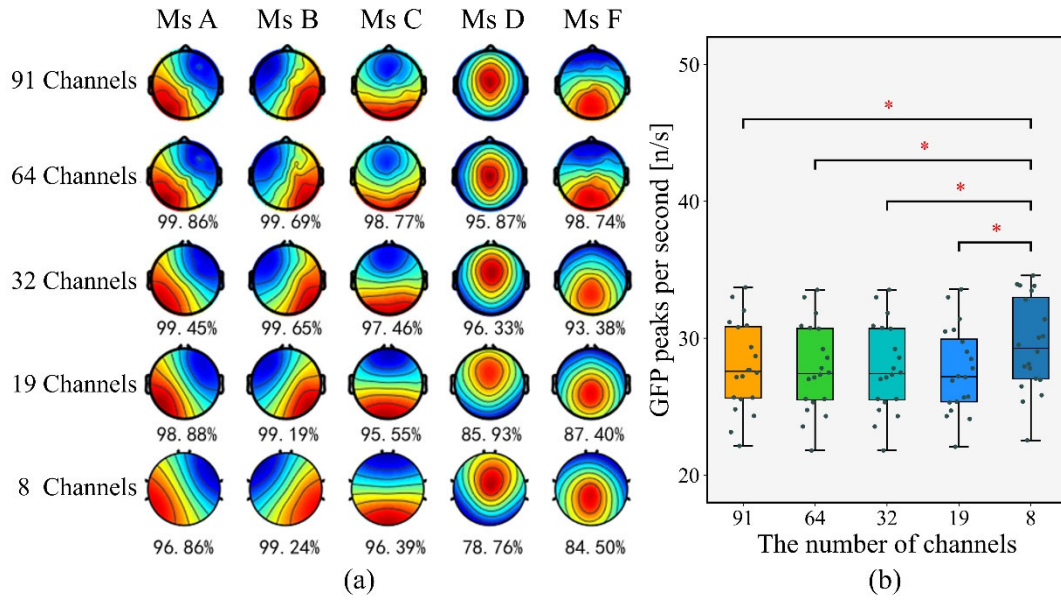


Fig. 4. (a) The topographies of MD microstates at five electrode densities. The maps were labeled as microstate A, B, C, D and F. The Pearson Correlation coefficients between microstate at 64, 32, 19, and 8 channels and corresponding microstate at 91 channels were marked under the topographies. (b) Boxplots of GFP peaks per second in MD condition at different electrode densities. The bar of each subgraph is the standard deviation. Ms: Microstate. *:p<0.005 (Bonferroni Corrected).

In MD condition, five sets of microstate maps are shown in Fig.4 (a). The PCC of microstates D and F were less than 0.9 in 19-channel configuration and the PCC of microstate D was less than 0.8 in 8-channel configuration. Fig.4 (b) reports the results of GFP peaks per second in MD condition. Compared with the BS condition, the value of GFP peaks per second fluctuated more violently in MD condition (range from 27.63 to 29.53). The statistical analysis showed that GFP peaks per second under 8 electrodes configuration have significant differences with GFP peaks per second under the other four configurations.

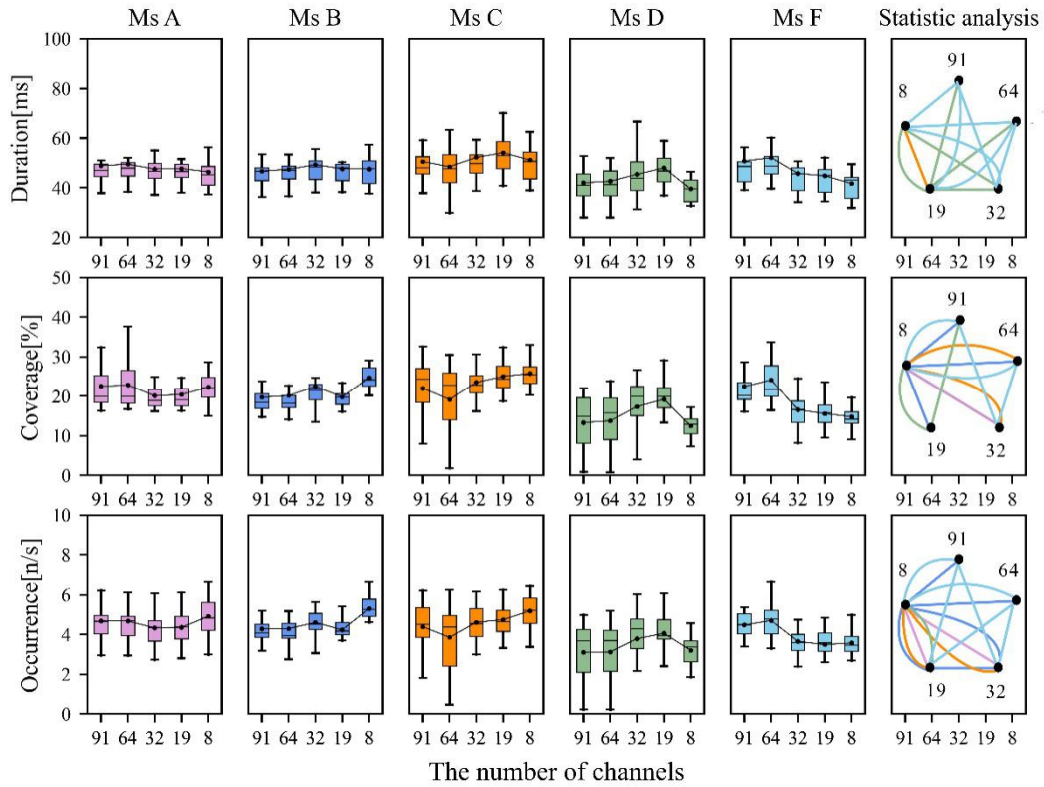


Fig. 5. Group comparison of (a) Duration, (b) Coverage, and (c) Occurrence in MD at different channel numbers. The five columns on the left are the mean-standard deviation graphs of microstate parameter. The right-most column is the result of statistics analysis. A line between two nodes indicates that these two configuration have significant differences and the color of the line mark the corresponding microstate. The bar of each subgraph is the standard deviation. All statistical differences have been Bonferroni Corrected. Ms: Microstate.

The descriptive statistics and ANOVA results of Duration, Coverage, and Occurrence are depicted in Fig. 5. Except for the differences between 32-channel configuration and 64-channel, 91-channel configurations in the microstate F, the other differences were all from between 19-channel or 8-channel configurations and the other configurations.

Table 2 Descriptive summary of ICC and CV results in MD condition

Parameter	ms	91vs64vs32vs19vs8		91vs64vs32vs19		91vs64vs32	
		ICC	CV	ICC	CV	ICC	CV
Duration	A	0.96	7.03%	0.96	6.27%	0.96	5.49%
	B	0.99	4.43%	0.99	4.13%	0.98	4.48%
	C	0.96	8.83%	0.94	9.15%	0.94	8.28%
	D	0.92	10.53%	0.92	9.86%	0.92	9.00%
	F	0.94	11.98%	0.95	10.23%	0.95	9.11%
Coverage	A	0.85	15.27%	0.85	15.17%	0.86	14.16%
	B	0.89	14.70%	0.94	11.33%	0.94	10.96%
	C	0.74	22.26%	0.74	23.29%	0.77	23.65%
	D	0.83	32.22%	0.84	30.53%	0.87	28.96%
	F	0.65	30.01%	0.64	28.83%	0.65	25.58%
Occurrence	A	0.95	9.29%	0.96	8.10%	0.95	7.72%
	B	0.9	12.39%	0.96	7.42%	0.96	6.84%
	C	0.84	19.37%	0.83	19.63%	0.85	21.10%
	D	0.88	26.92%	0.88	26.57%	0.9	24.74%
	F	0.69	19.71%	0.68	20.21%	0.68	18.30%
STD		0.1	8.51%	0.11	8.77%	0.1	8.35%
Average		0.87	16.33%	0.87	15.38%	0.88	14.56%

2

3 Table 2 shows the descriptive summary of ICC and CV in MD condition. The average
4 ICC and CV of 5KED were 0.87 (SD=0.10) and 16.33% (SD=8.51%). The average ICC
5 and CV of 4KED was 0.87 (SD=0.11) and 15.38% (SD=8.77%). The average ICC and
6 CV of 3KED was 0.88 (SD=0.10) and 14.56% (SD=8.35%). Statistical analysis showed
7 that the ICC of 3KED was significantly different from that of 4KED and 5KED.
8 Combining numerical and statistical analysis result, the consistency was high at 91, 64,
9 32 channels, and when 19, 8 was introduced, the consistency decreased.

10 The Transition Probability results at MD condition are shown in Fig. S3. For all 25

1 different microstate transitions in MD condition, results between 91 and 64 channels
2 were still stable. As the electrode density decreases, the stability of the parameter results
3 decreases, and the significant difference between the results at different electrode
4 densities increases. The ICC and CV of Transition Probability in MD condition are
5 shown in Table S2. The results of ICC and CV of Transition Probability compared to
6 the basic parameters are poor, and ICC is lower and CV is higher at the same electrode
7 density combinations. However, the consistency of 3KED is still higher than that of
8 5KED. The results of the entropy rate in MD condition are shown in Fig. S4. Entropy
9 Rate could remain stable at greater than 19 channels and significant change at 8
10 channels, which is consistent with the result in the BS condition.

11

12 *3.3 Comparison during propofol-induced transition of consciousness*

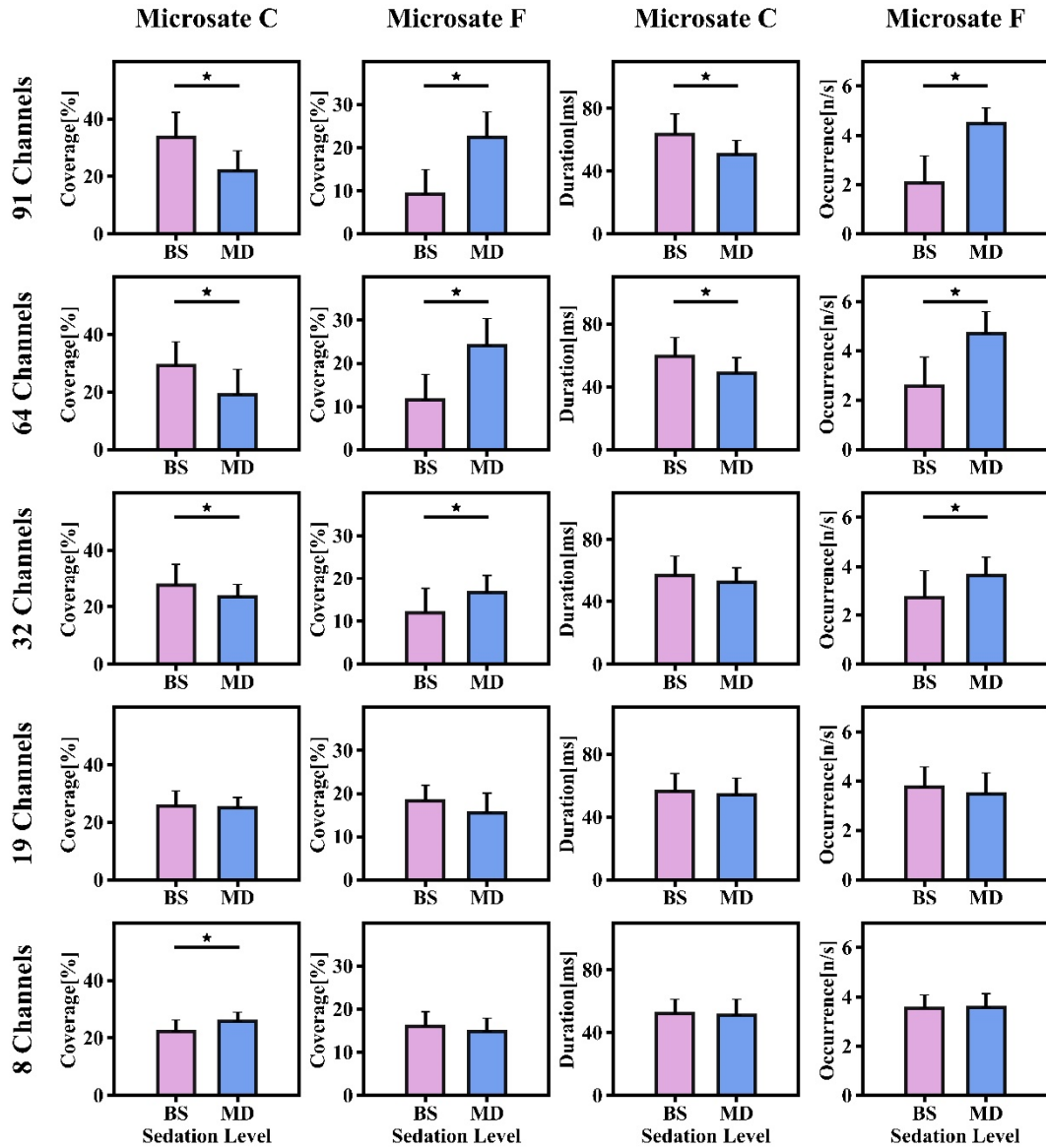


Fig. 6. Comparison of Coverage C, Coverage F, Duration C, and Occurrence F between BS and MD conditions during the change of consciousness under different electrode densities. The bar of each subgraph is the standard deviation. Significant differences were marked in the figures. All statistical differences have been Bonferroni Corrected

Fig. 6 depicts the comparison of four microstate four basic parameters in BS and MD conditions. Under 91 electrodes configuration, there were significant differences between two conditions for all four parameters and these result were in line with expectation. Under 64 and 32 electrodes configurations, most of the differences between BS and MD conditions remained stable. However, under 19 and 8 electrodes

configurations, Similar significant differences with high electrode density disappeared. Not only that, Coverage C showed the opposite significant difference under 8 channels. Similarly, the comparison of sequence-related parameters at BS and MD conditions has shown in Fig. S5. The transition probability of microstates A to C, B to C, D to C, and F to C at 91 channels is significant different between the BS and MD conditions. Repeated comparison shows that the part of the differences has disappeared at 19 channels and 8 channels.

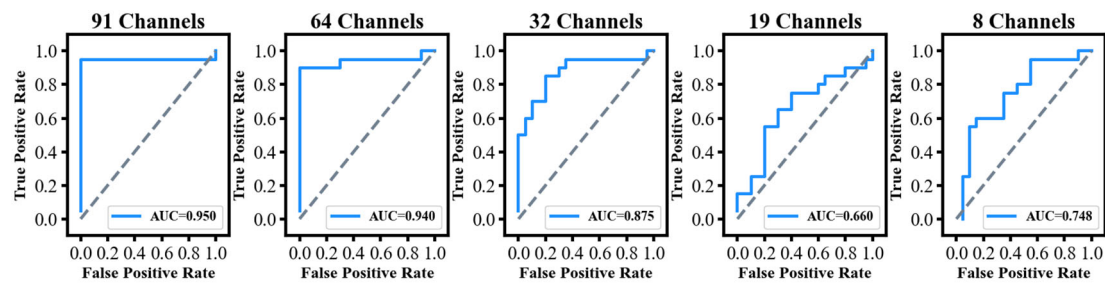


Fig. 7. The ROC curve of SVM classification between BS and MD was shown in right-most column. The area under curves (AUC) was calculated and marked in the graphs. BS: baseline, MD: moderate sedative, ROC: receiver operating characteristic, AUC: area under curve.

Eight parameters that had significant difference between BS and MD conditions was input as features to perform svm classification in 91, 64, 32, and 19 channels. However, seven parameters were input in 8 channels because the Coverage C has the opposite difference at 8 channels. The ROC curves obtained by SVM classifier with parameters are shown in the Fig. 7. The AUC of classification at 91, 64, 32, 19 and 8 electrodes configuration was 0.950, 0.940, 0.875, 0.660, and 0.748, and the classification accuracy is 97.5%, 92.5%, 80%, 65%, and 62.5% respectively. These results also demonstrated that distinguishability between BS and MD conditions decreased with the electrode density decreased.

1

2 **Table 3** The descriptive statistics summary of ICC during the propofol-induced transition

Parameter	ms	91vs64vs32vs19vs8		91vs64vs32vs19		91vs64vs32	
		mean	std	mean	std	mean	std
Duration	A	0.9	0.15	0.94	0.05	0.95	0.04
	B	0.94	0.06	0.96	0.03	0.95	0.04
	C	0.8	0.25	0.83	0.24	0.85	0.22
	D	0.8	0.16	0.82	0.24	0.86	0.2
	F	<i>0.78</i>	0.26	<i>0.78</i>	0.23	0.84	0.21
Coverage	A	<i>0.66</i>	0.32	<i>0.72</i>	0.35	<i>0.74</i>	0.35
	B	<i>0.59</i>	0.31	<i>0.74</i>	0.21	<i>0.73</i>	0.25
	C	<i>0.66</i>	0.25	<i>0.69</i>	0.27	<i>0.73</i>	0.22
	D	<i>0.67</i>	0.26	<i>0.72</i>	0.31	0.8	0.25
	F	<i>0.55</i>	0.34	<i>0.67</i>	0.28	0.81	0.17
occurrence	A	0.82	0.22	0.89	0.11	0.88	0.13
	B	<i>0.74</i>	0.28	0.81	0.27	0.8	0.3
	C	<i>0.73</i>	0.24	<i>0.79</i>	0.22	<i>0.77</i>	0.23
	D	<i>0.66</i>	0.34	<i>0.69</i>	0.37	<i>0.74</i>	0.34
	F	<i>0.59</i>	0.31	<i>0.68</i>	0.3	<i>0.79</i>	0.22

3

4 The consistency results of five different electrode densities in four conditions for each
5 subject are shown in Table 3. The averaged ICC of 5KED (10 parameters) and 4KED
6 (9 parameters) were below 0.8. In 3KED, only 6 ICCs were below 0.8. When comparing
7 only three electrode densities with no less than 32 channels, the consistency of the
8 microstate parameters is optimal.

9

10 **Discussion**

11 The spatial analysis of EEG using microstates has been widely utilized to reveal the
12 specific neural mechanisms in the process of brain state changes. However, it still

1 remains unknown whether the electrode density will affect the reliability of microstate
2 analysis. For example, our previous high-density EEG research showed that,
3 associated with default mode network, the microstate C has been found to undergo
4 some changes during the transition of consciousness, but it is not certain whether low-
5 density EEG can detect this change. In this study, the reliability of microstates at
6 different electrode densities was tested during the propofol-induced transition of
7 consciousness and it is expected that the minimum recommended number of electrodes
8 will be provided for further microstate analysis. Based on previously analyzed 91-
9 channel dataset, five datasets with different electrode densities were converted by
10 manually removing some channels. The following information will discuss the stability
11 of microstate topography, the microstate parameter in one condition, and the microstate
12 features between different conditions at different electrode densities.

13 The correlation of microstate topographies between different electrode densities is
14 different between BS and MD conditions. In the BS condition, as taking 91-channel
15 microstates as the templates, all microstates of 64, 32, 19, or 8 channels have had the
16 excellent PCC. The microstates A, B, C, and D is a group of typical microstates that are
17 stable in resting state and can be generally recognized in most studies using different
18 electrode densities (Khanna et al., 2015; Michel and Koenig, 2017). The topographic
19 map of microstates A, B, C, and D explained more global variance than other special
20 microstates (Custo et al., 2017). However, in the MD condition, as the number of
21 channels decreased, the PCC decreased to below 0.9, or even below 0.8 in certain
22 situations. We think that the difference in clustering number may be a reason for
23 variation as mentioned in some earlier studies (Lai, 1988; Murray et al., 2008). In the
24 MD condition, because the clustering number is set to 5, compared with four stable
25 microstates, a new microstate with a small proportion reduces the difference between
26 the classes, which could cause each sampling point more likely to be clustered into
27 different classes under different electrode configurations (Pascual-Marqui, 1995).
28 According to the result, the microstates D and F are mainly affected. The larger
29 difference in the number of channels, the greater possibility of class changes. In
30 particular, the cluster center maps of microstates D and F under 8 channels varied

greatly compared with that of 91 channels. In the meantime, an interesting phenomenon is that the 64-channel microstate F looks more like the Class C than the microstate C visually. However, the results of Pearson correlation coefficient showed that the 64-channel microstate C and the 91-channel microstate C have the highest correlation (0.987), but the Pearson correlation coefficient between 64-channel microstates F and 91-channel microstate C is 0.843. Therefore, how to label on microstates will also have an impact on the result, and it is necessary to have a relatively normative standard. There is also a certain difference in the 91-channel microstate D between BS and MD conditions. The difference may come from the number of clusters. When the number of clusters is 5, microstates D and F with high similarity can be distinguished. When the number of clusters is 4, microstates D and F are combined into one cluster. In addition, for the same dataset, different numbers of channels are selected for clustering, and the results are not completely consistent. Then, for different datasets, the clustering results must be more different. Therefore, although microstates in different research results have the same labels, there are some differences in terms of the topography (Gschwind et al., 2016; Seitzman et al., 2017), so it will potentially affect the consistency of conclusion. This may be one of the explanations for the inconsistent conclusions of multiple studies on schizophrenia. Therefore, in order to ensure clinical application value, the number of channels with stable results should be selected for microstate analysis.

At present, most of existing studies about the microstate mainly focus on the comparison of parameters (Drissi et al., 2016; Tomescu et al., 2015). The number and position of GFP peaks in EEG data play an important role in the microstate analysis (Mishra et al., 2020). The process of clustering and microstate fitting is based on the data corresponding to the GFP peaks position (Corradini and Persinger, 2014). Therefore, if the number and position of GFP peak points vary a lot at different electrode densities, the clustering microstate and parameters will be affected greatly. In BS and MD conditions, although the numerical distribution showed little change under five electrode configurations, statistical analysis revealed a significant difference between 8

1 channels and the other numbers of channels. Therefore, the dataset corresponding to the
2 GFP peaks at the 8-channel configuration must be partly inconsistent with the dataset
3 at other configurations. As a consequence, different conclusions may be drawn on
4 dataset with 8 channels compared with other datasets.

5
6 Also, in BS and MD conditions, the reliability of Duration, Coverage, Occurrence,
7 Transition Probability, Entropy Rate at five electrode densities was also measured. The
8 stability of the Entropy Rate is high, and the results under no less than 19 leads are very
9 stable. The numerical distributions of Duration, Coverage, Occurrence are not as
10 consistent as GFP peaks per second. The result was expected as existing studies had
11 shown that parameters of healthy subjects (Khanna et al., 2014) or schizophrenics
12 (Rieger et al., 2016) have had differences with different channel numbers. Statistics
13 analysis showed that there were few significant differences between the parameters of
14 91, 64, and 32 channels, and the differences mainly existed between 19, 8, and other
15 channels. This result indicated that the parameters using less than 20-channel might
16 have low stability. When the electrode density was low, different results would be
17 produced at different number of channels. ICC and CV are commonly used indicators
18 when evaluating reliability. Here, we used them to measure the consistency of
19 microstate parameters calculated at different electrode densities. The consistency of
20 parameter was quantified by ICC and CV. The ICC and CV of 5KED, 4KED and
21 3KED were calculated in BS and MD conditions. The result showed that the
22 consistency between 91, 64 and 32 channels was excellent, but consistency decreases
23 when 19 channels and 8 channels were introduced successively. The reliability of
24 Transition Probability at different electrode densities is worse than basic parameters. In
25 the MD condition, the partial Transition Probability of 32 channels is inconsistent with
26 the transition probability at higher electrode density. The decrease in parameter
27 consistency at the low electrode density may be due to the inconsistency between the
28 dynamic process of the brain state recorded at low channel number and the recording
29 at high channel number. In other words, the description of topographic maps under
30 different electrode densities is different. For example, when the electrode density is low,

an EEG electrode records a “characteristic signal” that can explain the current brain state. Due to the low electrode density and the long distance between the electrodes, the surrounding electrodes cannot detect this “characteristic signal”. If this electrode is removed, the energy at the corresponding position of the topographic map will be replaced by the smoothed average value of the surrounding electrodes, resulting in the loss of this information that can reveal current brain activity. Then, the same sampling point may be labeled into a different cluster, which affects the parameter calculation. However, when the electrode density is high enough, the same position may be covered by more than one electrode, but the addition and deletion of partial electrodes will not affect the topographic map. Therefore, a more convincing parameter result can be obtained by selecting a high electrode density for microstate analysis. In addition, compared with the microstates A and B, with distinctive features in the spatial structure, the spatial structures of the microstates C, D, and F are relatively similar, and it makes the results of ICC and CV of the microstate C, D, and F are worse than that of microstates A and B.

Microstate, as an emerging biomarker, has been extensively used to compare features between consciousness-related conditions or participant groups (Comsa et al., 2019; Strik et al., 1995). We have found that the microstate parameters change as electrode density changes. In order to evaluate if the microstate was a reasonable biomarker, we also tested the reliability of microstate features between different brain states. Eight parameters had significant differences between BS and MD conditions. If these differences were stable, it could also be observed in other electrode configuration. The results showed that the microstate features at 64 and 32 channels revealed the same differences as those at 91 channels, but part of differences disappeared at 19 and 8 channels. The statistical analysis results of microstate features are similar to that of microstate parameters. The application of microstate features in classification has a broad prospect, and it is of great significance to the diagnosis of diseases and the monitoring of brain state. If we can not get the same result at different electrode densities, it will be impractical in clinical diagnosis. The classification results of four

1 microstate parameters showed that the less the number of channels, the worse the
2 classification performance. The ICC of parameters between four conditions also
3 showed that the consistency of 91, 64, and 32 channels was better. Therefore, the
4 microstate features between different brain states remained stable and reliable at higher
5 electrode densities. Based on the above results, the consistency and stability of
6 microstate features between different brain states were guaranteed when the number of
7 channels was no less than 32.

8
9 Also, this study has some limitations to assess the reliability of the microstate. We only
10 studied the reliability of the microstate in sedation. Whether the reliability of other task
11 state is consistent with that of sedation needs further study. Similarly, only the electrode
12 configuration was tested to see whether it could affect the consistency of the microstate,
13 while the influence of other factors, such as smoothing parameter and preprocessing
14 strategies, remains to be studied.

16 **Conclusion**

17 The present study analyzed the influence of channel number on microstate analysis and
18 provided the recommended number of channels for further microstate research. In this
19 study, the reliability of microstate at different electrode densities was investigated. First,
20 the reliability of microstate topography and parameters was measured in the baseline
21 condition and the moderate condition, respectively. Second, the reliability of microstate
22 feature differences during propofol-induced transitions of brain states was measured.
23 The results showed that microstate analysis at 91, 64, and 32 channels showed the high
24 inter-state and intra-state reliability and consistency. Conclusions obtained using low
25 electrode density could not be reproducible with high electrode density. When
26 conducting microstate analysis, it is recommended to use no less than 32-channel EEG
27 data, and the channels should be evenly distributed on the scalp.

28 **Conflicts of interest**

29 The authors declare no competing financial interests.

1

2 **Acknowledgments**

3 This work was supported in part by the National Natural Science Foundation of China
4 under Grants 32071372, 31571000 and 61471291; in part by the Natural Science Basic
5 Research Program of Shaanxi under Program No. 2020JM-037; and in part by the
6 Fundamental Research Funds for the Central Universities of China under Grant
7 xjj2017122.

8

9 **Reference**

- 10 Brandeis, D., Lehmann, D., Michel, C.M., Mingrone, W., 1995. Mapping event-related brain potential
11 microstates to sentence endings. *Brain Topogr* 8, 145-159.
- 12 Britz, J., Van De Ville, D., Michel, C.M., 2010. BOLD correlates of EEG topography reveal rapid resting-
13 state network dynamics. *Neuroimage* 52, 1162-1170.
- 14 Brodbeck, V., Kuhn, A., von Wegner, F., Morzelewski, A., Tagliazucchi, E., Borisov, S., Michel, C.M., Laufs,
15 H., 2012. EEG microstates of wakefulness and NREM sleep. *Neuroimage* 62, 2129-2139.
- 16 Chennu, S., O'Connor, S., Adapa, R., Menon, D.K., Bekinschtein, T.A., 2016. Brain Connectivity Dissociates
17 Responsiveness from Drug Exposure during Propofol-Induced Transitions of Consciousness. *PLoS*
18 *Comput Biol* 12, e1004669.
- 19 Comsa, I.M., Bekinschtein, T.A., Chennu, S., 2019. Transient Topographical Dynamics of the
20 Electroencephalogram Predict Brain Connectivity and Behavioural Responsiveness During Drowsiness.
21 *Brain Topogr* 32, 315-331.
- 22 Corradini, P.L., Persinger, M.A., 2014. Spectral power, source localization and microstates to quantify
23 chronic deficits from 'mild' closed head injury: correlation with classic neuropsychological tests. *Brain*
24 *Inj* 28, 1317-1327.
- 25 Custo, A., Van De Ville, D., Wells, W.M., Tomescu, M.I., Brunet, D., Michel, C.M., 2017.
26 Electroencephalographic Resting-State Networks: Source Localization of Microstates. *Brain Connect* 7,
27 671-682.
- 28 Drissi, N.M., Szakacs, A., Witt, S.T., Wretman, A., Ulander, M., Stahlbrandt, H., Darin, N., Hallbook, T.,
29 Landtblom, A.M., Engstrom, M., 2016. Altered Brain Microstate Dynamics in Adolescents with
30 Narcolepsy. *Front Hum Neurosci* 10, 369.
- 31 Fitzgerald, P.J., Watson, B.O., 2018. Gamma oscillations as a biomarker for major depression: an
32 emerging topic. *Translational psychiatry* 8, 177.
- 33 Grieder, M., Koenig, T., Kinoshita, T., Utsunomiya, K., Wahlund, L.O., Dierks, T., Nishida, K., 2016.
34 Discovering EEG resting state alterations of semantic dementia. *Clin Neurophysiol* 127, 2175-2181.
- 35 Gschwind, M., Hardmeier, M., Van De Ville, D., Tomescu, M.I., Penner, I.K., Naegelin, Y., Fuhr, P., Michel,
36 C.M., Seeck, M., 2016. Fluctuations of spontaneous EEG topographies predict disease state in relapsing-
37 remitting multiple sclerosis. *Neuroimage Clin* 12, 466-477.
- 38 Gudmundsson, S., Runarsson, T.P., Sigurdsson, S., Eiriksdottir, G., Johnsen, K., 2007. Reliability of
39 quantitative EEG features. *Clin Neurophysiol* 118, 2162-2171.

1 Ip, C.T., Ganz, M., Ozenne, B., Sluth, L.B., Gram, M., Viardot, G., l'Hostis, P., Danjou, P., Knudsen, G.M.,
2 Christensen, S.R., 2018. Pre-intervention test-retest reliability of EEG and ERP over four recording
3 intervals. *Int J Psychophysiol* 134, 30-43.

4 Katayama, H., Gianotti, L.R., Isotani, T., Faber, P.L., Sasada, K., Kinoshita, T., Lehmann, D., 2007. Classes
5 of multichannel EEG microstates in light and deep hypnotic conditions. *Brain Topogr* 20, 7-14.

6 Khanna, A., Pascual-Leone, A., Farzan, F., 2014. Reliability of resting-state microstate features in
7 electroencephalography. *PLoS One* 9, e114163.

8 Khanna, A., Pascual-Leone, A., Michel, C.M., Farzan, F., 2015. Microstates in resting-state EEG: current
9 status and future directions. *Neurosci Biobehav Rev* 49, 105-113.

10 Kikuchi, M., Koenig, T., Munesue, T., Hanaoka, A., Strik, W., Dierks, T., Koshino, Y., Minabe, Y., 2011. EEG
11 microstate analysis in drug-naïve patients with panic disorder. *PLoS One* 6, e22912.

12 Kikuchi, M., Koenig, T., Wada, Y., Higashima, M., Koshino, Y., Strik, W., Dierks, T., 2007. Native EEG and
13 treatment effects in neuroleptic-naïve schizophrenic patients: time and frequency domain approaches.
14 *Schizophr Res* 97, 163-172.

15 Koenig, T., Prichep, L., Lehmann, D., Sosa, P.V., Braeker, E., Kleinlogel, H., Isenhardt, R., John, E.R., 2002.
16 Millisecond by millisecond, year by year: normative EEG microstates and developmental stages.
17 *Neuroimage* 16, 41-48.

18 Laganaro, M., 2017. Inter-study and inter-Individual Consistency and Variability of EEG/ERP Microstate
19 Sequences in Referential Word Production. *Brain Topogr* 30, 785-796.

20 Lai, W.J.K.T., 1988. A Criterion for Determining the Number of Groups in a Data Set Using Sum-of-Squares
21 Clustering. *Biometrics* 44, 23-34.

22 Lehmann, D., Faber, P.L., Galderisi, S., Herrmann, W.M., Kinoshita, T., Koukkou, M., Mucci, A., Pascual-
23 Marqui, R.D., Saito, N., Wackermann, J., Winterer, G., Koenig, T., 2005. EEG microstate duration and
24 syntax in acute, medication-naïve, first-episode schizophrenia: a multi-center study. *Psychiatry Res* 138,
25 141-156.

26 Lehmann, D., Ozaki, H., Pal, I., 1987. EEG alpha map series: brain micro-states by space-oriented
27 adaptive segmentation. *Electroencephalogr Clin Neurophysiol* 67, 271-288.

28 Michel, C.M., Koenig, T., 2017. EEG microstates as a tool for studying the temporal dynamics of whole-
29 brain neuronal networks: A review. *Neuroimage* 180, 577-593.

30 Michel, C.M., Koenig, T., 2018. EEG microstates as a tool for studying the temporal dynamics of whole-
31 brain neuronal networks: A review. *Neuroimage* 180, 577-593.

32 Milz, P., Pascual-Marqui, R.D., Achermann, P., Kochi, K., Faber, P.L., 2017. The EEG microstate topography
33 is predominantly determined by intracortical sources in the alpha band. *Neuroimage* 162, 353-361.

34 Mishra, A., Englitz, B., Cohen, M.X., 2020. EEG microstates as a continuous phenomenon. *Neuroimage*
35 208, 116454.

36 Murray, M.M., Brunet, D., Michel, C.M., 2008. Topographic ERP analyses: a step-by-step tutorial review.
37 *Brain Topogr* 20, 249-264.

38 Musso, F., Brinkmeyer, J., Mobascher, A., Warbrick, T., Winterer, G., 2010. Spontaneous brain activity
39 and EEG microstates. A novel EEG/fMRI analysis approach to explore resting-state networks.
40 *Neuroimage* 52, 1149-1161.

41 Nishida, K., Morishima, Y., Yoshimura, M., Isotani, T., Irisawa, S., Jann, K., Dierks, T., Strik, W., Kinoshita,
42 T., Koenig, T., 2013. EEG microstates associated with salience and frontoparietal networks in
43 frontotemporal dementia, schizophrenia and Alzheimer's disease. *Clin Neurophysiol* 124, 1106-1114.

44 Pascual-Marqui, R.D., Michel, C. M., & Lehmann, D. , 1995. Segmentation of brain electrical activity into

1 microstates: model estimation and validation. *IEEE Transactions on Biomedical Engineering* 42, 658-665.

2 Rieger, K., Diaz Hernandez, L., Baenninger, A., Koenig, T., 2016. 15 Years of Microstate Research in

3 Schizophrenia - Where Are We? A Meta-Analysis. *Front Psychiatry* 7, 22.

4 Seitzman, B.A., Abell, M., Bartley, S.C., Erickson, M.A., Bolbecker, A.R., Hetrick, W.P., 2017. Cognitive

5 manipulation of brain electric microstates. *Neuroimage* 146, 533-543.

6 Sharmila, A., 2018. Epilepsy detection from EEG signals: a review. *J Med Eng Technol* 42, 368-380.

7 Shi, W., Li, Y., Liu, Z., Li, J., Wang, Q., Yan, X., Wang, G., 2020. Non-Canonical Microstate Becomes Salient

8 in High Density EEG During Propofol-Induced Altered States of Consciousness. *Int J Neural Syst* 30,

9 2050005.

10 Shoukri, M.M., Colak, D., Kaya, N., Donner, A., 2008. Comparison of two dependent within subject

11 coefficients of variation to evaluate the reproducibility of measurement devices. *BMC Med Res*

12 *Methodol* 8, 24.

13 Shrout, P.E., Fleiss, J.L., 1979. Intraclass correlations: uses in assessing rater reliability. *Psychological*

14 *bulletin* 86, 420-428.

15 Skrandies, W., 1990. Global field power and topographic similarity. *Brain Topogr* 3, 137-141.

16 Strelets, V., Faber, P.L., Golikova, J., Novototsky-Vlasov, V., Koenig, T., Gianotti, L.R.R., Gruzelier, J.H.,

17 Lehmann, D., 2003. Chronic schizophrenics with positive symptomatology have shortened EEG

18 microstate durations. *Clinical Neurophysiology* 114, 2043-2051.

19 Strik, W.K., Dierks, T., Becker, T., Lehmann, D., 1995. Larger topographical variance and decreased

20 duration of brain electric microstates in depression. *Journal of neural transmission. General section* 99,

21 213-222.

22 Tomescu, M.I., Rihs, T.A., Roinishvili, M., Karahanoglu, F.I., Schneider, M., Menghetti, S., Van De Ville, D.,

23 Brand, A., Chkonia, E., Eliez, S., Herzog, M.H., Michel, C.M., Cappe, C., 2015. Schizophrenia patients and

24 22q11.2 deletion syndrome adolescents at risk express the same deviant patterns of resting state EEG

25 microstates: A candidate endophenotype of schizophrenia. *Schizophr Res Cogn* 2, 159-165.

26 von Wegner, F., Knaut, P., Laufs, H., 2018. EEG Microstate Sequences From Different Clustering

27 Algorithms Are Information-Theoretically Invariant. *Frontiers in Computational Neuroscience* 12.

28 von Wegner, F., Tagliazucchi, E., Laufs, H., 2017. Information-theoretical analysis of resting state EEG

29 microstate sequences - non-Markovianity, non-stationarity and periodicities. *Neuroimage* 158, 99-111.

30 Zappasodi, F., Croce, P., Giordani, A., Assenza, G., Giannantoni, N.M., Profice, P., Granata, G., Rossini,

31 P.M., Tecchio, F., 2017. Prognostic Value of EEG Microstates in Acute Stroke. *Brain Topogr* 30, 698-710.

32